









Experimental and Metamodel Based Optimization of Cutting Parameters for Milling Inconel-800 Superalloy Under Nanofluid MQL Condition

Ngoc-Chien Vu¹, Huu-That Nguyen¹, Van-Han Nguyen¹, Quang-Nhu Phan¹, Ngoc-Thai Huynh², Xuan-Phuong Dang^{1*}

¹ Faculty of Mechanical Engineering, Nha Trang University, No.2 Nguyen Dinh Chieu St., Vinh Tho Dist., Nha Trang City, Khanh Hoa 650000, Vietnam

² Faculty of Mechanical Technology, Ho Chi Minh City University of Food Industry, 31 Che Lan Vien, Tay Thanh Ward, Tan Phu District, Ho Chi Minh 700000, Vietnam

Corresponding Author Email: phuongdx@ntu.edu.vn

<https://doi.org/10.18280/mmep.100121>

ABSTRACT

Received: 29 October 2022

Accepted: 23 January 2023

Keywords:

superalloy material, nanofluid MQL, approximation, optimization, environment friendly machining

Machining of Inconel-800, a superalloy material that is difficult-to-cut materials, has received the special attention of many scientists worldwide. This paper adopts the advanced and industry-accepted lubrication method that is minimum quantity lubrication technique (MQL) which enhances nanoparticle particles to improve the machinability of Inconel-800 superalloy material and reduce the quantity of conventional cutting fluids. The metamodel namely Radial basis function (RBF) was used for expressing the relationship between cutting velocity, feed per tooth, depth of cut, and corner radius to two quality factors, including cutting force and specific cutting force. A combination of the RBF approximate model and Non-dominated Sorting Genetic Algorithm II (NSGA-II) algorithm was applied to find out optimal global solutions for the multi-objective optimization problem. The results show that this study plays a part in supporting scientists and engineers to understand machining difficult-to-cut materials better and minimize waste to the environment towards sustainable and environmentally friendly machining.

1. INTRODUCTION

With the development of engineering materials, difficult-to-cut materials were born to meet the different requirements of each specific field [1]. Inconel-800 super-alloy is one of the typical hard-to-cut materials. The outstanding features of the material can be mentioned as superior toughness, tremendous tensile strength, immeasurable corrosion resistance, and high-temperature strength always attract users to find suitable machining methods to increase the machinability. So, the machining difficult-to-cut materials also revealed a concern for scientists and engineers [2].

The minimum quantity lubrication (MQL) cooling technique uses very small amounts of cutting fluids (50 - 500 mL/h) that are delivered to the cutting zone as a mist cooling under the required increased air pressure changing from 2 to 6 bar from the nozzle [3]. MQL is an effective cooling technique that is of interest to scientists. A technological breakthrough was made to further enhance fluid cutting properties by using minuscule solids particles (less than 100 nm) to add to the cutting fluid or lubrication in 1995 [4]. That cooling technique is called nanofluid MQL, for which Choi is the originator. From then on, a broad research direction for researchers has been developed in applying nanoparticles for minimum quantity lubrication machining [5]. The invention of nanoparticle-based cutting fluid in the machining process support overcoming the weakness of cutting fluids increases thermal conductivity, density, and viscosity of the cutting fluids. It also significantly enhances the heat transfer process

in the cutting zone in machining [6].

Many materials have extensively studied the investigation and modelling of cutting force properties [7, 8]. However, studying the influence of parameters on cutting force for newly Inconel-800 superalloy material is also challenging for researchers, and there are few articles written on the topic. In addition, multi-objective optimization with opposing objects, including cutting force, specific cutting force, and material removal rate, is also worth discussing.

According to the literature currently available [8-11], studies on modeling and optimizing process parameters for multi-objectives in the field of metal processing focus on the manufacturing industries. Response Surface Methodology (RSM), artificial neural network (ANN), Kriging model, and RBF are the most common models used to illustrate the interaction between input and output parameters. Because of its versatility and dependability, RBF is the most widely used by engineering researchers.

There are various techniques commonly employed in engineering to tackle the optimization problem. Some generic optimization approaches, such as Taguchi [8, 12] and Grey Relational Analysis (GRA) [13, 14], are used in metal cutting; nevertheless, these techniques cannot provide optimal results with a "really optimal" solution considering that they only optimize depending on the level of control factors. Mia and co-authors [15, 16] typically employ the desirability function technique for simultaneous multi-response optimization. They used a satisfying function technique for multi-objective optimization of various cutting circumstances, such as dry, wet,

cryogenic cooling, and MQL. Because revolution optimization techniques are adequate, flexible, easy, and compelling, researchers have steadily used them to handle multi-objective optimization problems. The Archive-based Micro Genetic Algorithm (AMGA) [17], genetic algorithm (GA) [18], PSO [6], and NSGA-II [19] are the optimization algorithms.

Consequently, our investigation employed the RBF approximate model to model the relationship between parameters and machining response. The Al₂O₃ nanofluid MQL enhances the machining of difficult-to-cut materials (Inconel-800 superalloy). In addition, the application of evolutionary optimization (NSGA-II) methods combines the RBF model to boost the optimal study to generate the solutions for machining difficult-to-cut materials.

2. MATERIAL AND METHODOLOGY

The material worked in this study is Inconel-800 super-alloy material which has exceptional properties as mentioned in the Introduction section. The cutting tool is a flat-end mill with a diameter of 16 mm and two Sandvik Coromant inserts, as shown in Figure 1. According to the theory of metal cutting, the three most essential factors that impact the product quality are cutting velocity, feed per tooth, and depth of cut. Based on the recommendation of the cutting parameters on the CoroPlus® Tool Guide website, the practical range of cutting velocity (v_c), depth of cut (a_p), and feed per tooth (f_z) are 90–150 m/min, 0.4–1 mm, and 0.03–0.09 mm/tooth, respectively. The geometry of the cutting tool (the insert) has three options for tool nose radius (0.4, 0.8, and 1.2 mm). To save the experiment time and cost, the design of the experiment (DOE) with an orthogonal array (Taguchi array) was employed. Each factor or input parameter was divided into three levels: lower (level 1), middle (level 2), and upper (level 3), with their values as shown in Table 1. The number of experiments and the combination of values of the cutting parameters were generated based on the L27 Taguchi array, as shown in Table 2. Each row of the experiment was repeated three times, and the average value of the machine responses was calculated to obtain reliable results.

Table 1. The input parameters and their levels

Input parameters	Unit	Level		
		1	2	3
Cutting velocity (v_c)	m/min	90	120	150
Feed per tooth (f_z)	mm/tooth	0.03	0.06	0.09
Depth of cut (a_p)	mm	0.4	0.7	1.0
Corner radius (r)	mm	0.4	0.8	1.2

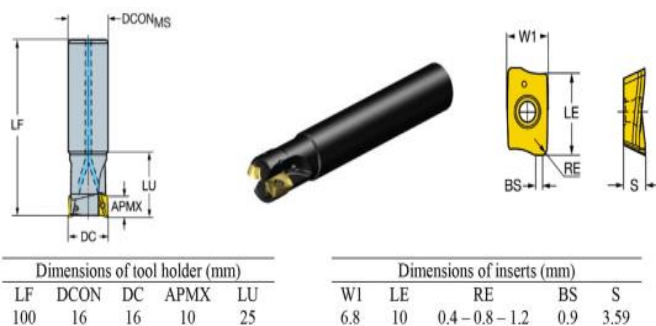


Figure 1. Cutting tool of Sandvik Coromant were used for the entire experiment

The response parameters we selected are cutting force (F_c), specific cutting force (K_s), and material removal rate (MRR). F_c was measured with Vishay Precision Group equipment. MRR can be determined according to the following formula.

$$MRR = \frac{1000 * a_p * a_e * v_c * f_z * z}{3.14 * d} \quad (1)$$

where, a_e is the width of cut (mm), z is the flute of milling tool, and d is diameter of milling tool (mm).

The formula carried out the computation of specific cutting force (K_s) shown in Eq. (2).

$$K_s = \frac{F_c}{S} = \frac{F_c}{f_z * a_p} \quad (2)$$

where, S is the section of chip layer [20].

The cooling and lubricating condition using MQL in this work is fixed. Al₂O₃ nanoparticles, which enhance the cutting condition, were utilized and dissolved into CT232 cutting oil commercialized in Taiwan. The nanoparticle concentration by volume mixed was 0.5% and was stirred for a minimum of 12 hours, as shown in Figure 2, to form a homogeneous mixture before experimenting.

The MQL parameters applied as flow rate, nozzle angle, the pressure of air, and nozzle distance stabilize at 90 mL/h, 60 degrees, 3 kg/cm², and 25 mm, respectively [6]. The experiment setup was arranged as shown in Figure 3.



Figure 2. Magnetic stirrer utilizes for mixing nanoparticles into CT232 cutting oil

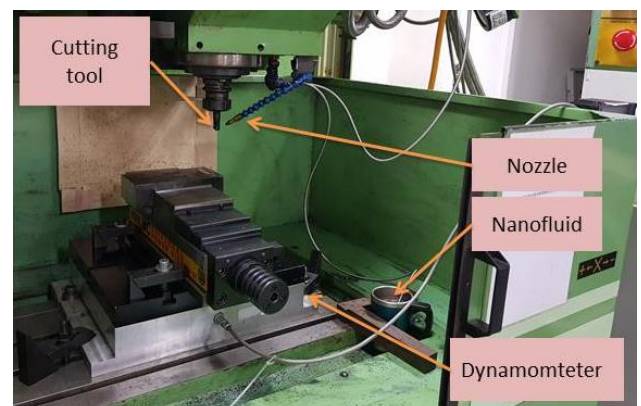


Figure 3. Experimental setup

The three-axis milling machine used to conduct the whole experiment is named Victor Vertical Machining Center 4. Slot milling and axial depth of cut is the type of milling the author employs. Figure 4 shows the experiment of milling operation running with nanofluid MQL. Figure 5 shows the workpiece after milling and testing with cutting parameters, as in Table 1 above.



Figure 4. Milling operation running with nanofluid MQL

The approximate RBF model combines with NSGA-II for modeling and optimization of technological parameters during machining. RBF approximation is a kind of neural network applying a hidden layer of radial units and an output layer of linear units. RBF approximations are used by reasonably fast training and reasonably compact networks. NSGA-II algorithm is one of the most commonly employed multi-objective optimization algorithms in engineering. This algorithm has features such as a high-speed non-dominated sorting approach, a crowded distance estimation procedure,

and an easily crowded comparison operator.

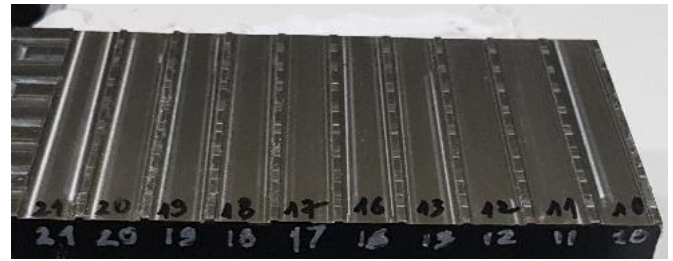


Figure 5. Finished workpiece Inconel-800 machined with nanofluid MQL

3. RESULTS AND DISCUSSION

The results of 27 experiments are tabulated in Table 2. Subsequently, the RBF approximation model was employed to capture the relationship between input and output parameters. The goodness of fit or fidelity of the RBF model is measured by the coefficient of the determinant (R-squared). Figure 6 shows the coefficient R^2 of the RBF model in this work. If the observed values lie on the diagonal line, there will be no error between the observed values and the predicted value, and the R-squared equals 1. The results of this work show that the R-squared of the RBF model for cutting force (Figure 6(a)) and specific cutting force (Figure 6(b)) are 0.93 and 0.94, respectively. The values of R-squared are pretty high and acceptable for engineering because they are higher than 0.9. As a result, the fidelity of the approximate model is excellent and significant.

Table 2. DOE and results of physical experiments

No	Input parameters			Radius of the cutting tool r (mm)	Response parameters		
	Cutting velocity v_c (m/min)	Depth of cut a_p (mm)	feed per tooth f_z (mm/tooth)		Cutting force F_c (N)	Material removal rate MRR (mm ³ /min)	Specific cutting force K_s (N/mm ²)
1	90	0.4	0.03	0.4	102.6	688	8550
2	150	0.4	0.09	0.4	372.6	3440	10350
3	120	0.4	0.06	0.4	253.4	1834	10558
4	120	0.7	0.03	0.4	242.0	1605	11524
5	150	0.7	0.06	0.4	480.0	4013	11429
6	90	0.7	0.09	0.4	249.0	3612	3952
7	150	1.0	0.03	0.4	383.5	2866	12783
8	90	1.0	0.06	0.4	285.2	3440	4753
9	120	1.0	0.09	0.4	546.4	6879	6071
10	120	0.4	0.03	0.8	158.1	917	13175
11	150	0.4	0.06	0.8	318.5	2293	13271
12	90	0.4	0.09	0.8	229.4	2064	6372
13	150	0.7	0.03	0.8	368.8	2006	17562
14	90	0.7	0.06	0.8	289.1	2408	6883
15	120	0.7	0.09	0.8	491.2	4815	7797
16	90	1.0	0.03	0.8	244.1	1720	8137
17	120	1.0	0.06	0.8	542.5	4586	9042
18	150	1.0	0.09	0.8	853.8	8599	9487
19	150	0.4	0.03	1.2	210.2	1147	17517
20	90	0.4	0.06	1.2	165.5	1376	6896
21	120	0.4	0.09	1.2	277.0	2752	7694
22	90	0.7	0.03	1.2	205.0	1204	9762
23	120	0.7	0.06	1.2	393.5	3210	9369
24	150	0.7	0.09	1.2	593.0	6019	9413
25	120	1.0	0.03	1.2	389.8	2293	12993
26	150	1.0	0.06	1.2	692.8	5733	11547
27	90	1.0	0.09	1.2	433.2	5159	4813

In Figure 7, the distribution of effects on cutting force is arranged as follows cutting velocity, depth of cut, feed per tooth, and radii of the cutting tool. Based on Eq. (2), we can also capture that depth of cut and feed per tooth are two factors affecting specific cutting forces. This rule can also be caught in Figure 8; when the depth of cut and feed per tooth increases, the specific cutting force decreases. K_s falls substantially, which is suitable for machining since it supports the milling cutting tool avoid breaking.

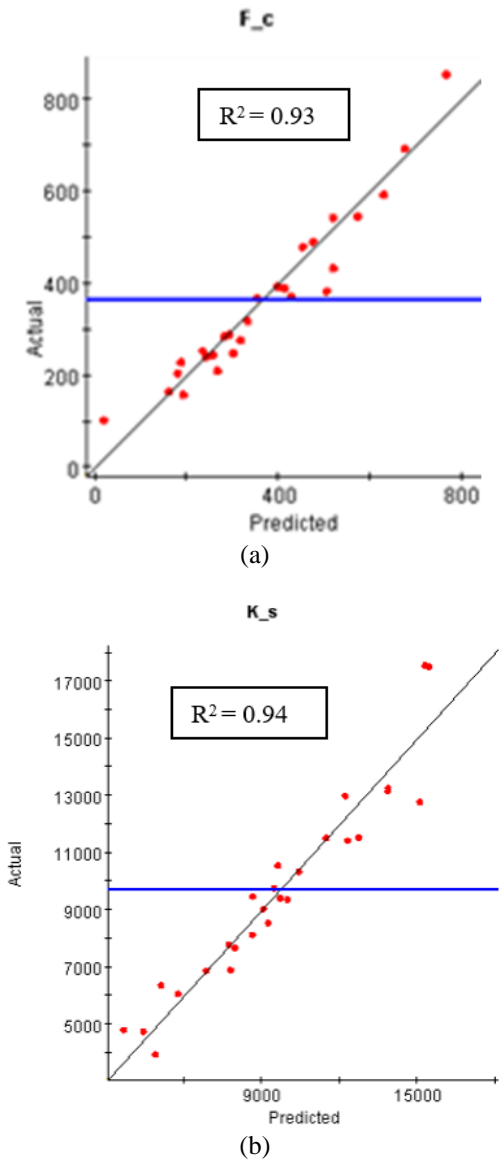


Figure 6. Coefficient R^2 of RBF model for cutting force (a) and specific cutting force (b)

The relationship between the cutting parameters and the machining responses modeled by the radial basis function approximation method is graphically shown in Figure 9. It can be seen that the increase in the value of cutting parameters increases cutting force. However, those relationships are non-linear.

When cutting velocity is combined with a high value of cutting depth, the cutting force increases sharply (Figure 9(a)). On the contrary, if the value of cutting depth is low, the increase in cutting force when increasing the cutting velocity is lower compared to the previous case. The influence of cutting nose radius and cutting feed per tooth is lower than that of cutting velocity and depth of cut (Figure 9(b) and Figure 7).

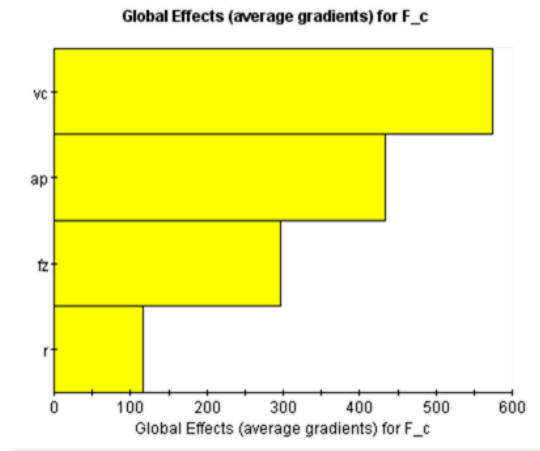


Figure 7. Global effect of milling parameters to cutting force

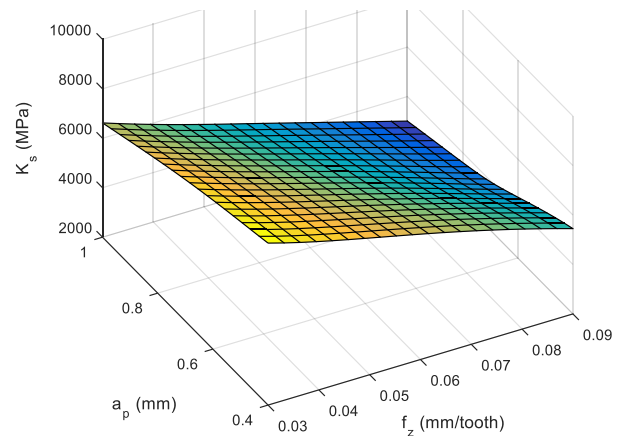


Figure 8. The response surface plot for specific cutting force

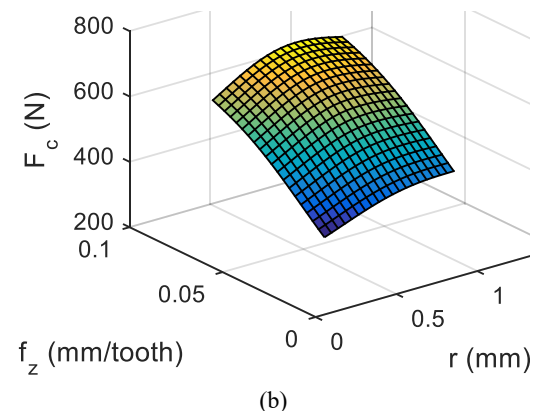
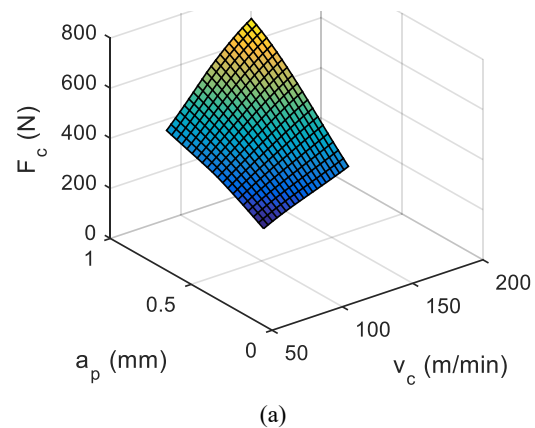


Figure 9. The response surface plot for cutting force (a, b)

When increasing feed per tooth and depth of cut, K_s decreases significantly, which is suitable in the machining process because it will assist the cutting tool to circumvent cracking during machining. However, when we increase the feed per tooth, F_c also raises; obviously, the bigger the F_c , the worse it is. It is undesirable in machining. So we need to optimize to compromise between F_c and K_s . Another goal to aim for is to maximize the MRR . So this is a multi-objective optimization problem where the outputs conflict with each other. We need to make compromises to create an optimal value for all three responses. So, the adequacy and significance of the RBF approximate model combined with the NSGA-II algorithm were employed for multi-objective optimization for maximum MRR , minimum cutting force and specific cutting force. The Pareto front shows the optimal results that can be observed in Figure 10.

The Pareto plots in Figure 10(a) and 10(b) shows all the possible solutions (both black and blue points) based on the Non-sorting Genetic Algorithm II when solving the optimization problem. All the points in the plot are feasible solutions. However, only the lowest points (blue points on the graph) measured in the vertical direction (because we solved the minimization problem) are the so-called Pareto optimal set. The Pareto plot provides the best trade-off solution for response parameters.

Indeed, cutting with a high material removal rate in the processing materials is always emphasized. However, high material removal rate means large cutting forces, which is not good. Therefore, if those two goals conflict, a reasonable compromise is needed. However, it is shown in Figure 10(b) that not every increase in MRR will increase K_s ; here, there is a suitable value of K_s (3020.2 N/mm², minimum value) corresponding to that of MRR (5320.5 (mm³/min)). The material removal rate, cutting force, and specific cutting force can choose a different value depending on the circumstances of the engineer or machine operator using the Pareto plot chart. Based on this, it can be seen that the relationship between the three output variables is quite complicated, so if the operator chooses according to experience or the operation guide, it will be challenging to find the optimal point for multi-objective optimization as the requirements of this study. This relationship can also be easily seen when skimming Figure 10(c), where the relationship of F_c , K_s , and MRR is most apparent. The compromises between three response factors are also easily selected, supporting engineers and manufacturers to optimize the desired response parameters.

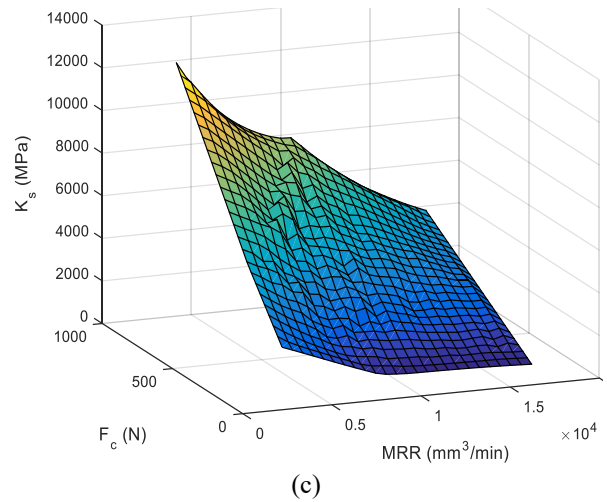
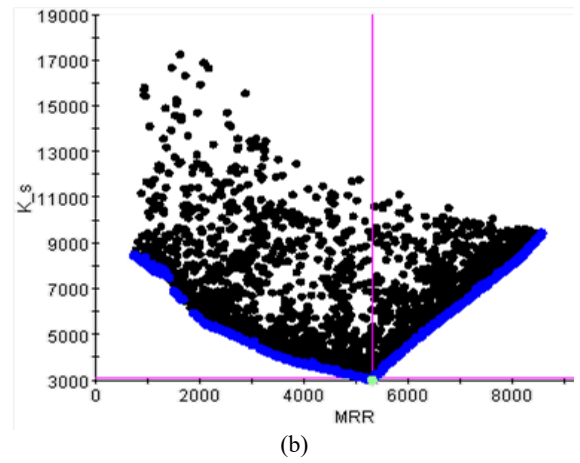
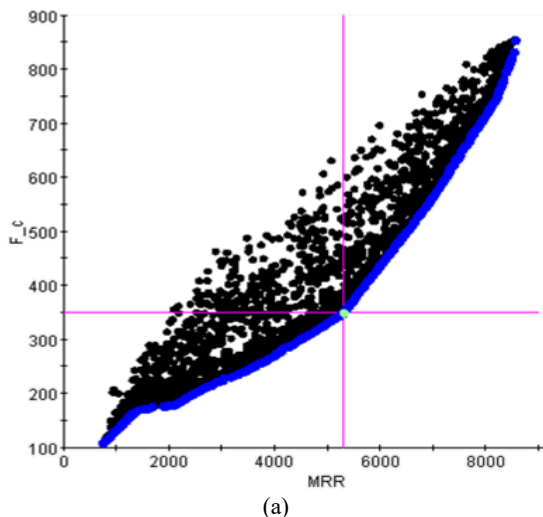


Figure 10. Pareto plot for cutting force, specific cutting force and MRR based on RBF model combined with NSGA-II (a, b, c)

4. CONCLUSION

The study approaches the employ of nanofluid MQL to support the machining of newly difficult-to-machine materials, which is Inconel-800 superalloy material. The paper also modeled and optimized the machining parameters in terms of cutting force, specific cutting force, and material removal rate. The application of Al₂O₃ nanoparticle assists in increasing the tribology of cutting oil which enhances the cutting efficiency. Following remarks can be drawn:

- i. The RBF is an appropriate metamodel that can accurately capture the approximate relationship between machining parameters and machining responses because of the high value of the R^2 coefficient in this work.
- ii. The work describes the relationship between input parameters and each output response in detail, clearly, and statistically.
- iii. Combining the RBF approximate model with the NSGA-II contributes to a proper solution for adversarial multi-objective optimization.
- iv. Pareto plot presented in this study makes it easier and more systematic to select cutting parameters (output and input parameters).
- v. The relationship between F_c , K_s , and MRR is built with effortless observation and high confidence.

ACKNOWLEDGMENT

The paper is sponsored by Nha Trang University under project No. TR2021-13-20.

REFERENCES

- [1] Şirin, Ş., Sarıkaya, M., Yıldırım, Ç.V., Kıvak, T. (2021). Machinability performance of nickel alloy X-750 with SiAlON ceramic cutting tool under dry, MQL and hBN mixed nanofluid-MQL. *Tribology International*, 153: 106673. <https://doi.org/10.1016/j.triboint.2020.106673>
- [2] Hsiao, T.C., Vu, N.C., Tsai, M.C., Dang, X.P., Huang, S.C. (2020). Modeling and optimization of machining parameters in milling of INCONEL-800 super alloy considering energy, productivity, and quality using nanoparticle suspended lubrication. *Measurement and Control*, 54(5-6): 42. <https://doi.org/10.1177/0020294020925842>
- [3] Do, T.V., Vu, N.C., Nguyen, Q.M. (2018). Optimization of cooling conditions and cutting parameters during hard milling of AISI H13 steel by using Taguchi method. 2018 IEEE International Conference on Advanced Manufacturing (ICAM), Yunlin, Taiwan, pp. 396-398. <https://doi.org/10.1109/AMCON.2018.8615057>
- [4] Chol, S.U.S., Estman, J.A. (1995). Enhancing thermal conductivity of fluids with nanoparticles. *ASME International Mechanical Engineering Congress and Exposition*, 231: 99-106.
- [5] Raja, M., Vijayan, R., Dineshkumar, P., Venkatesan, M. (2016). Review on nanofluids characterization, heat transfer characteristics and applications. *Renewable Sustainable Energy Reviews*, 64: 163-173. <https://doi.org/10.1016/j.rser.2016.05.079>
- [6] Vu, N.C., Dang, X.P., Huang, S.C. (2020). Multi-objective optimization of hard milling process of AISI H13 in terms of productivity, quality, and cutting energy under nanofluid minimum quantity lubrication condition. *Measurement and Control*, 54(5-6): 57. <https://doi.org/10.1177/0020294020919457>
- [7] Filho, S.L.M.R., Pereira, R.B.D., Lauro, C.H., Brandão, L.C. (2019). Investigation and modelling of the cutting forces in turning process of the Ti-6Al-4V and Ti-6Al-7Nb titanium alloys. *The International Journal of Advanced Manufacturing Technology*, 101(9): 2191-2203. <https://doi.org/10.1007/s00170-018-3110-7>
- [8] Vu, N.C., Huang, S.C., Nguyen, H.T. (2018). Multi-objective optimization of surface roughness and cutting forces in hard milling using Taguchi and response surface methodology. *Key Engineering Materials*, 773: 220-224. <https://doi.org/10.4028/www.scientific.net/KEM.773.220>
- [9] Park, H.S., Nguyen, T.T., Dang, X.P. (2016) Multi-objective optimization of turning process of hardened material for energy efficiency. *International Journal of Precision Engineering Manufacturing*, 17(12): 1623-1631. <https://doi.org/10.1007/s12541-016-0188-4>
- [10] Selaimia, A.A., Yallese, M.A., Bensouilah, H., Meddour, I., Khattabi, R., Mabrouki, T. (2017). Modeling and optimization in dry face milling of X2CrNi18-9 austenitic stainless steel using RMS and desirability approach. *Measurement*, 107: 53-67. <https://doi.org/10.1016/j.measurement.2017.05.012>
- [11] Prakash, C., Singh, S., Pabla, B.S., Sidhu, S.S., Uddin, M.S. (2019). Bio-inspired low elastic biodegradable Mg-Zn-Mn-Si-HA alloy fabricated by spark plasma sintering. *Materials and Manufacturing Processes*, 34(4): 357-368. <https://doi.org/10.1080/10426914.2018.1512117>
- [12] Vu, N.C., Huynh, N.T., Huang, S.C. (2019). Optimization the first frequency modal shape of a tensural displacement amplifier employing flexure hinge by using Taguchi Method. *Journal of Physics: Conference Series*, 1303: 012016. <https://doi.org/10.1088/1742-6596/1303/1/012016>
- [13] Vu, M.H., Huynh, N.T., Nguyen, K.N., Tran, A.S., Nguyen, Q.M. (2022). Optimal stress and strain of helical gear and rack in the steering system. *Mathematical Modelling of Engineering Problems*, 9(3): 697-706. <https://doi.org/10.18280/mmep.090316>
- [14] Huynh, N.T., Huang, S.C., Dao, T.P. (2018). Optimal displacement amplification ratio of bridge-type compliant mechanism flexure hinge using the Taguchi method with grey relational analysis. *Microsystem Technologies*, 27: 1251-1265. <https://doi.org/10.1007/s00542-018-4202-x>
- [15] Mia, M. (2018). Mathematical modeling and optimization of MQL assisted end milling characteristics based on RSM and Taguchi method. *Measurement*, 121: 249-260. <https://doi.org/10.1016/j.measurement.2018.02.017>
- [16] Mia, M. (2017). Multi-response optimization of end milling parameters under through-tool cryogenic cooling condition. *Measurement*, 111: 134-145. <https://doi.org/10.1016/j.measurement.2017.07.033>
- [17] Nguyen, T.T. (2019). Prediction and optimization of machining energy, surface roughness, and production rate in SKD61 milling. *Measurement*, 136: 525-544. <https://doi.org/10.1016/j.measurement.2019.01.009>
- [18] Liang, F.S., Yan, G.P., Fang, F.Z. (2022). Global time-optimal B-spline feed rate scheduling for a two-turret multi-axis NC machine tool based on optimization with genetic algorithm. *Robotics Computer-Integrated Manufacturing*, 75: 102308. <https://doi.org/10.1016/j.rcim.2021.102308>
- [19] Vu, N.C., Truong, T.T., Nguyen, H.T. (2022). Experimental Investigation of Cutting Parameters in Machining of Inconel-800 Super-Alloy Under Nanofluid MQL Using Integrated RSM and NSGA-II. *Cham, Springer International Publishing*, 192-198. https://doi.org/10.1007/978-3-030-99666-6_30
- [20] Aouici, H., Elbah, M., Benkhelladi, A., Fnides, B., Boulanouar, L., Yallese, M.A. (2019). Comparison on various machinability aspects between mixed and reinforced ceramics when machining hardened steels. *Mechanics & Industry*, 20(1): 109. <https://doi.org/10.1051/meca/2018052>